

INTEREST- INTERnational REMote Student Training at JINR University Center
Joint Institute for Nuclear Research
Dubna, Moscow region, Russian Federation

The Wave5 project report:
**Coexistence of superconductivity and ferromagnetism at low-dimensional
heterostructures**

Student
Jovana Vlahović

Supervisor
Dr. Vladimir Zhaketov

November 2021.

Contents

Abstract	3
1. Introduction	3
1.1. Superconductivity.....	3
1.2. Ferromagnetism.....	5
1.3. Proximity effects in superconductor-ferromagnet structures	7
1.4. Neutron reflectometry	9
1.5. X-ray reflectivity	10
1.6. Task 2. Comparing reflectivity at different grazing angles (calculation only neutron reflectivity).....	11
1.7. Task 3. Comparing reflectivity at different magnetization (calculation only neutron reflectivity).....	13
1.8. Task 4. Comparing structures with different thicknesses (calculation of neutron and X-ray reflectivity).....	16
1.9. Task 5. Comparing structures with different ferromagnets (calculation of neutron and X-ray reflectivity).....	18
1.10. Task 6. Superlattice (calculation of neutron and X-ray reflectivity)	20
1.11. Task 7. Influence of roughness (calculation only X-ray reflectivity).....	22
2. Conclusion	23

Abstract

One of the good, powerful, and helpful techniques for analyzing the superconducting/ferromagnet proximity effect in low-dimensional heterostructures. Here, we investigated the $\text{Al}_2\text{O}_3/\text{Nb}(100\text{nm})/\text{Gd}(3\text{nm})/\text{V}(70\text{nm})/\text{Nb}(15\text{nm})$ heterostructures. Due to the interaction of neutrons with nuclei and magnetic moments we can discuss the influence of the grazing angle of the neutron beam, colinear and non-collinear magnetization, the thickness of the ferromagnetic layer, different ferromagnetic materials, size of the superlattice, and roughness of the structure on the reflectivities spectra. By comparing the different values of mentioned properties and different ferromagnetic materials, we conclude that there is a mutual influence of the ferromagnetic and superconducting layers in analyzed heterostructures.

1. Introduction

The idea of the possible coexistence of the superconductivity (S) and ferromagnetism (F) in the one layer of a heterostructure is based on the possibility of pairing electrons from different layers which are next to each other. This phenomenon is very interesting and hard to explain. It depends on many different causes and conditions, such as elemental profile and magnetic profile of the heterostructure, the roughness of a surface of the layers, the thickness of superconducting layers, temperature, the strength of the external magnetic field, etc.

In this report, the influence of different structural and experimental parameters on the proximity and inverse proximity effects in S-F low-dimensional heterostructures will be investigated by neutron reflectometry with detecting secondary radiation.

1.1. Superconductivity

The Dutch physicist Heike Kamerlingh Onnes revealed a new intriguing phenomenon in 1911. He researched cooling techniques and noticed that on temperatures below 4.15K the resistance of mercury dropped to zero. This was the first time that someone reached the superconductivity state.

Superconductivity is a phenomenon characterized by the disappearance of electrical resistance in various materials, alloys, and compounds when cooled below the appropriate temperature known as the critical temperature T_c when occurs the phase transition between the normal and superconductive state of an examined sample. On temperatures below T_c , during the flow of a constant electric current, the behavior of a superconductor is as if it has no electrical resistance at all, $\rho = 0$, Figure 1. For temperatures above T_c these materials have normal properties of a usual conductor, $\rho \gg 0$. The superconductor, therefore, behaves as an ideal diamagnetic. Inside the superconductor, the electric field is $E = \rho J = 0$, and with these materials, the current appears to exist only on the surface. An electric current through the superconducting wire in the shape of a loop can persist indefinitely without any power source.

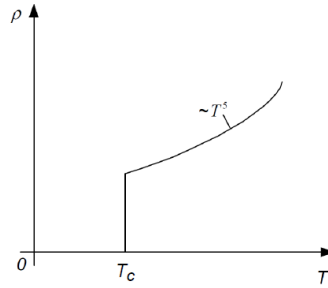


Figure 1. Temperature dependence of the electrical resistance.

In addition to the abrupt decrease in the specific electrical resistance to zero, it was observed that at temperatures below T_c , the superconductor placed in the external magnetic field expels the magnetic flux from itself. The left side of Figure 2 shows the conductor in the ordinary state (above T_c) and on the right side the superconducting state (below T_c). This phenomenon is called the Meissner effect, according to a scientist who discovered it in 1933, and is explained by the induction of surface superconducting currents which cancel out the external ones with their field. It is good to note that there is a dependence of the critical magnetic field on the temperature, Figure 3.

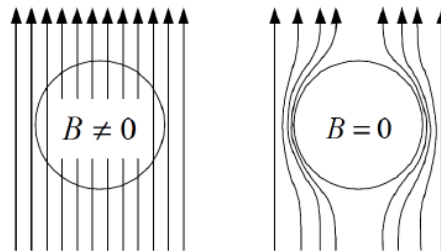


Figure 2. The behavior of the material's normal-conductive state at the left side and the Meissner effect in the superconductor state.

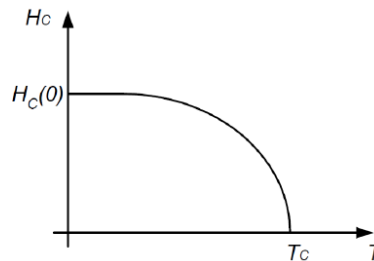


Figure 3. Dependence of H_c of temperature.

There are also limit values of current density J and magnetic field B . In 1913, Onnes found that superconductive states occur just below a critical current density J_c and it gets destroyed if the current density increase above it. Subsequently to this, he showed that there is also a limit in value of magnetic field - critical magnetic field B_c . At temperatures below T_c , in the superconductor located in the magnet field less than a B_c , there is an electric current just on the surface of the material. The magnetic field of this current completely compensates the applied external field $B = \mu_0 \mu_r H = 0$ and $\mu_r = 1 + X_m$. Critical magnetic field decreases monotonically with the increasing of the temperature and on the critical temperature disappears. It is concluded that some material

can be in a superconductive state under the conditions $T < T_c$, $J < J_c$, and $B < B_c$ ($H < H_c$) (TJB/TJH area), Figure 4.

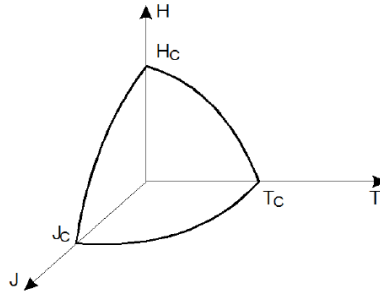


Figure 4. Schematic diagram of superconductive TJH area.

Through the decades, the highest known T_c was around 23.2K for Nb_3Ge , which is why superconductors had to be cooled with liquid nitrogen. In 1986, scientists discovered a new class of high-temperature superconductors – superconductive ceramics. The value of their T_c can be higher than 100K so they can be cooled by liquid nitrogen (77.3K), which is much cheaper than liquid helium.

Superconductivity was discovered in 1911 but the first successful mathematical explanation was given by London brothers 24 years later. They set two equations, named by them, which explained the behavior of current density, electric and magnetic field in TJB area in superconductive materials. The important thing for this report, which they proposed is the penetration depth of the external magnetic field in the superconductor. Ginzburg and Landau proposed a new theory of superconductivity. They predicted that the existence of superconductivity is based on forming of pairs of super electrons which are called Cooper pairs. Based on this phenomenological theory, there are two types of superconductors. Type I superconductors exhibit the Meissner effect below critical values of B, J, and T and there is a clear phase transition from normal to superconductive phase on H_c . Type II superconductors have two critical values of magnetic field H_{c1} and H_{c2} . Above both H , the material is in the normal phase and below both, it is in superconductive phase and it exhibits the Meissner effect. But when the field is between these critical values, $H_{c1} < H < H_{c2}$ there is a mixture of these two phases. The magnetic field can penetrate partially into the superconductive material which consists of alternating normal and superconducting domains. This microstructure is called a mixed state.

Badreen, Cooper, and Schrieffer gave a microscopic theory of superconductivity (BSC theory) in 1957. First, they showed that superconductivity depends on the atomic mass of the elements in examined material which means that an isotopic effect occurs. So they concluded that the ionic lattice of the semiconductor actively participates in forming of superconductive state and that electron-phonon interactions represent an additional interaction that leads to the mutual attraction of electrons and the construction of electron pairs.

1.2. Ferromagnetism

Magnetism is a phenomenon that explains the attraction or repulsion between magnets and magnetized materials. All magnetic materials are composed of small magnetic dipoles which have two poles: northern and southern. Materials can be magnetized permanently (without the influence of external magnetic field) or they have just induced magnetization due to the presence of external magnetic field—induced magnetism. Based on the nature of the magnetization in materials,

magnetic materials are roughly divided into diamagnetism, paramagnetism, and ferromagnetism (and ferrimagnetism and antiferromagnetism).

Diamagnetism is the property of materials to form a magnetic field that is opposite to the external magnetic field. Without an external magnetic field, diamagnetic materials are not magnetized. This type of magnetism exists in all materials but it is really weak compared to other types. Magnetic dipoles of diamagnetics are antiparallel to an applied magnetic field, Figure 5. Paramagnetism is a form of magnetism that occurs only in the presence of an external magnetic field. Paramagnetic materials are attracted by the action of a magnetic field, but unlike ferromagnetic ones, they show magnetic properties exclusively in the presence of an external magnetic field. Magnetic dipoles of paramagnetic are randomly positioned outside of the magnetic field. In the applied field they are parallel to the field, Figure 5.

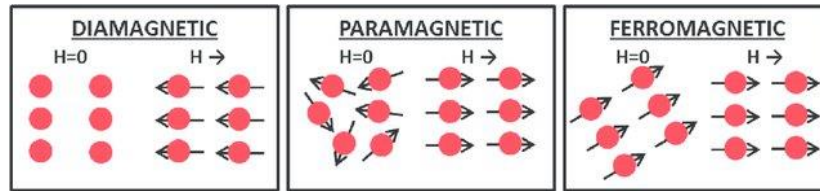


Figure 5. Orientation of magnetic dipoles with and without applied external field. From left to right: diamagnetic, paramagnetic and ferromagnetic material.

Ferromagnetic materials are naturally magnetic, they don't need an external field for inducing magnetization. This type of magnetism is the strongest one. Magnetic dipoles of a ferromagnet are distributed into small domains in which they are parallel to each other but magnet dipoles of different domains are positioned randomly to each other. Applying of external magnetic field forces magnetic dipoles in all domains to reorient and align with the field, Figure 5.

A characteristic of ferromagnetism is the S-shaped hysteresis curve, Figure 6, which describes the magnetization of ferromagnetic materials under the influence of an external magnetic field. The shape of this curve is a consequence of the magnetic direction of the electromagnet at the atomic level, and the direction of the magnetic domains measured in micrometers and nanometers. Magnetic hysteresis is a phenomenon in which the magnetization of a ferromagnetic body depends not only on the actual value of the magnetic field but also on previous magnetic states.

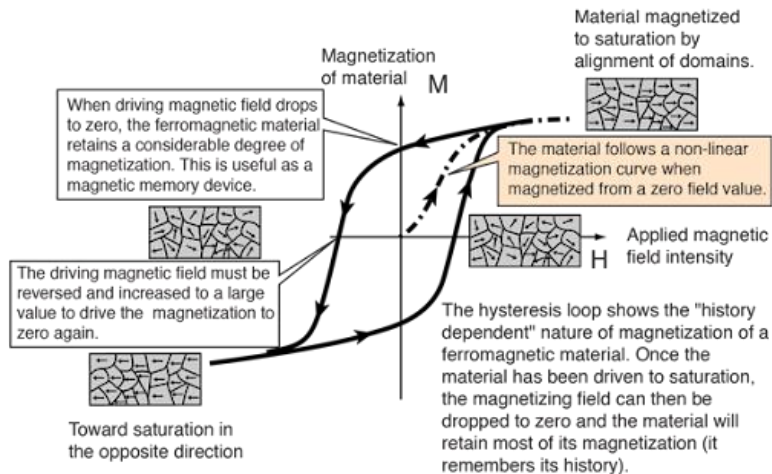


Figure 6. Hysteresis ferromagnetic curve. (<http://hyperphysics.phy-astr.gsu.edu/hbase/Solids/hyst.html>)

When the external magnetic field is removed, the domains are partially disoriented and the magnetization decreases. The ferromagnetic material shows the property of remanent magnetization. For the material to demagnetize, it is necessary to apply an external magnetic field in the opposite direction. The magnetic arrangement can be disrupted by heating. Then ferromagnetic materials become paramagnetic. The temperature at which the magnetic order of the material disappears is called the Curie temperature, T_c , Figure 7.

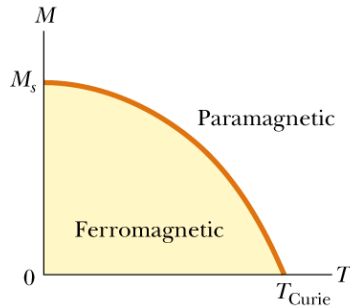


Figure 7. The transition from ferromagnetic to a paramagnetic arrangement on Curie temperature (<https://www.toppr.com/ask/content/concept/curies-law-271609/>).

The carriers of the elementary magnetic moments are electron spins. As with other solid-state magnetic phenomena, so with ferromagnetism, the magnetic forces are too weak to be responsible for the ordering of spins. The parallel arrangement of magnetic moments is also energetically unfavorable. The forces responsible for the ordering of spins are the so-called forces of change, which are related to the possible states of the two-electron system and the Pauli principle. It can be said that the ordering of magnetic moments is a consequence of the quantum mechanical force of change, and not of the classical magnetic force.

According to Pauli's principle, the asymmetric wave function of the position corresponds to the symmetric wave function of the spin. It can be shown that the mean distance of the particles is larger in the case of the asymmetric wave function of the position, and therefore the electrostatic repulsion force is lower for the same particles. The forces of change lead to an effective reduction of potential energy. Electrons with parallel spins, according to Pauli's principle, cannot remain in the ground state and must pass into a series of higher energy states, which increases their kinetic energy. The spontaneous parallel arrangement of magnetic spins, therefore, occurs when the decrease in potential energy is more than compensated by the increase in kinetic energies.

1.3. Proximity effects in superconductor-ferromagnet structures

When there are two different materials next to each other due to close contact they can affect each other. So the phenomena which originate from them (in the case of this research ferromagnetism and superconductivity) can affect each other, mix or coexist. This effect includes all interactions on the interface between two materials and in most cases, it is a consequence of the exchanging of electrons between two materials. Due to the superconductivity of one of these layers, we can call these pairs of electrons Cooper pairs.

On the surface (ie it can be said that in the contact area due to inhomogeneity of these structures) of the ferromagnetic and superconducting layer there is a mutual influence of ferromagnetism and superconductivity caused by the finite value of characteristic coherent length and London penetration depth. Change of the density of the superconductive electrons isn't fast, so there is a minimum length on which that change can occur without destroying of

superconductive state and it is called coherence length. The second fundamental length is related to the characteristic distance in which the magnetic field can penetrate into the superconducting region – London penetration depth λ_L . In the case of mutual interaction of ferromagnetism and superconductivity, two effects are defined: the proximity effect refers to the influence of the superconductivity on ferromagnetism, and the inverse proximity effect refers to the opposite affection of ferromagnetism on superconductivity. Both effects are the consequence of the interaction of free electrons in ferromagnetic material and conduction electrons in the superconducting layer close to the contact interface. These electrons are exchange-coupled. Occurred Cooper pairs of electrons induce superconductivity in a ferromagnetic material by penetration in it. In the exchange field, a ferromagnet the up-spin electron decreases its energy by h , while the down-spin electron energy increases by the same value. To compensate this energy variation, the up-spin electron increases its kinetic energy, while the down-spin electron decreases its kinetic energy.

Analyzed structures in this research are of nanometer dimensions and the F layers are several nanometers thick because the interplay between S and F phenomena occur at a nanometer scale. Also, in general, ferromagnetism is much "stronger" than superconductivity so it could destroy superconductivity by an exchange mechanism. But depending on conditions and temperature, both superconductivity and ferromagnetism can destroy one another. In the ferromagnetic state, the exchange field doesn't let electrons pair by aligning all Cooper pair spins in the same direction. This effect is called the paramagnetic effect. In addition to this effect, many different effects can occur in S/F systems. One of them is the cryptoferromagnetic effect which refers to the formation of nonuniform domain structure in the S layer. The coherence length is larger than the period of the domain ferromagnetic structure but the period is larger than the interatomic distance. It can be concluded that the period of occurrence of these domains is really small. The existence of the cryptomagnetic state is confirmed by showing that there occurred a decrease in the average magnetization in the F layer. One can say that domain structural organization is the consequence of the coexistence of ferromagnetism and superconductivity inside one same layer. It can be said that from the magnetic side it looks like ferromagnetism but from the superconductivity side like antiferromagnetism. Besides these effects many other can occur in the S/F structures, some of them are damped oscillatory behavior of the Cooper pair wave function in the ferromagnet, spatial oscillations of the electron density of states, a spontaneous vortex phase, π Josephson junctions in S/F/S systems, a nonmonotonic dependence of the T_c of S/F multilayers and bilayers on the ferromagnet layer thickness, and triplet superconductivity. Maybe the most important of them is the damped oscillatory behavior of the Cooper pair wave function in the ferromagnet which results in a nonmonotonic dependence of the T_c of S/F multilayers on the thickness of the ferromagnetic layer, as well as in the formation of π junctions in S/F/S interfaces.

It should be noted that the length of the interface of the F and S layers in investigated structures is comparable to the coherent lengths of superconductivity and ferromagnetism. Close to this interface occurs changing of properties of both layers. For the experimental study of these properties, electrical resistance and magnetic field (behaving of magnetic moments) are usually measured. But due to changes in the properties, spatial magnetic and superconducting profiles must be determined. They can be successfully measured by polarized neutron reflectometry.

1.4. Neutron reflectometry

Neutrons are noncharged particles of big mass and they have spin. They can interact with nuclei and penetrate deep into the sample. Due to their spin, they can interact with magnetic dipoles in the material so it is possible to obtain a spatial magnetic profile of the analyzed sample.

Neutron reflectometry is a technique for determining the structure of thin films based on neutron diffraction on the nuclei of the atoms in the analyzed structure. The sample is irradiated with a highly collimated neutron beam which reflects on it. The intensity of the reflected beam is being measured as a function of the angle of a wavelength of neutrons. From this dependence, it is possible to get information about the thickness, density, and roughness of the surface of the sample. Neutrons are especially suitable for use in analyzing the S/F structures due to that that thermal neutron wavelength corresponds to the characteristic coherent length and London penetration depth in superconductors and ferromagnets. Also, spatial profiles can be easily obtained due to the high penetration power of neutrons. Wavelengths of used neutrons for obtaining analyzed results are between 1 and 20 Å.

Measurement can be performed in specular and off-specular mode. In specular mode, the angle of the incident beam is equal to the angle of the reflected beam. Neutron reflection is described in terms of a momentum transfer vector Q :

$$Q = \frac{4\pi}{\lambda} \sin(\theta_i), \quad (1)$$

where λ is the neutron wavelength and θ_i the angle of the incident beam, Figure 8. The momentum transfer vector denotes the change of neutron momentum after reflection on the sample ($Q = k_i - k_f$, Figure 8). Off-specular reflectometry gives rise to diffuse scattering and involves momentum transfer within the layer, Figure 8, and is used to determine lateral correlations within the layers, such as those arising from magnetic domains or in-plane correlated roughness.

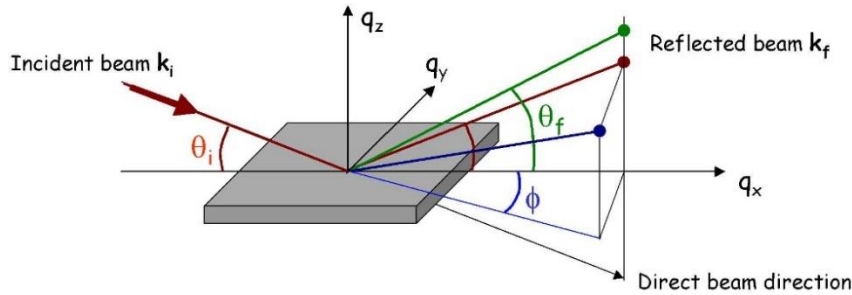


Figure 8. Scheme of the neutron reflection on the sample.

Standard polarized neutron reflectometry is used for determining the spatial magnetic profile. Neutrons can have two different polarizations in a magnetic field. The positive one is the direction of the applied magnetic field and the negative one is in a direction opposite to the magnetic field. Due to the different interactions of these neutrons with nuclei of the atoms in the heterostructure and the field, spin asymmetry and neutron polarizability can occur. So we can say that there are two states of neutrons, on the basis of which there can be four different reflectivities:

$$r = \begin{pmatrix} r_{++} & r_{+-} \\ r_{-+} & r_{--} \end{pmatrix}. \quad (2)$$

Magnetic moments of neutrons can be aligned in the direction of the magnetic field (+ state) and the opposite direction (- state).

Due to differences in values of reflectivities from Eq. 2., spin asymmetry can occur and it can be calculated by the following equation. The polarization of neutrons can be changed by spin flippers in the neutron spectrometer before and after the reflection on the sample.

$$\text{Spin asymmetry} = \frac{r_{++} - r_{--}}{r_{++} + r_{--}}. \quad (3)$$

In the heterostructures and on the interface between its layers, the interaction potential is the sum of the interaction potentials of all elements close to the interface which penetrate from one layer to another. So, it is not possible to obtain just by standard neutron reflectometry a good magnetic and elemental profile of the structure. For this, it is necessary to obtain the potential profile of the interaction of neutrons with all elements in the sample which is possible by registering secondary radiation too. In the neutron reflectivity experiment, the absorption can take place so we can say that sum of reflectivity and transmission is less than 1 so it is possible to analyze emitted particles or beams due to occurred absorption. It can give us additional information about the structure, already mentioned earlier.

Different types of radiation can be registered, but most common are charged particles, gamma quanta, and fission fragments which give more detailed information about the elemental/isotopic profile of the interface. Simultaneous registration of reflected neutrons and secondary radiation makes it possible to determine the good spatial profiles of isotopes in the examined material.

In S/F heterostructures, there is a modification of the magnetic and superconducting properties which affects the change in the spatial magnetic profile and distribution of the magnetization in the material so the neutron reflectivity is a powerful technique for determining these changes and is very useful for explaining the impact of these phenomena one to each other.

1.5. X-ray reflectivity

X-ray reflectivity is based on measuring the reflection of an X-ray beam from a surface in a specular direction which means that the angle of the reflected beam is equal to the angle of the incident beam, Figure 9. The surface of the material can be perfectly flat but if it isn't the reflection will deviate from that predicted by Fresnel's law of reflectivity. Due to this unevenness, analyzing the deviations, a surface density profile can be obtained.

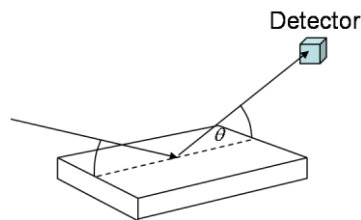


Figure 9. X-ray reflectivity (https://en.wikipedia.org/wiki/X-ray_reflectivity).

Below the critical angle of total external reflection, X-rays penetrate only a few nanometers into the sample. Above this angle, the penetration depth increases rapidly. At every interface where the electron density changes, a part of the X-ray beam is reflected. The interference of these partially reflected X-ray beams creates the oscillation pattern observed in reflectivity experiments, Figure 10. From reflectivity curves, one can determine layer parameters such as thickness and surface density gradients and layer density, interface, and surface roughness, Figure 10.

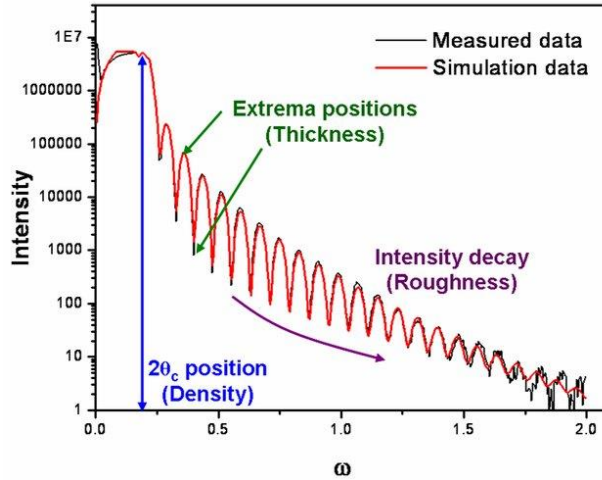


Figure 10. Typical XRR pattern of a thin film on a substrate. The density, thickness, and roughness of the film are obtained from the critical angle, period of oscillations, and intensity decay, respectively (https://www.researchgate.net/publication/27560704_Influence_of_deposition_parameters_on_morphology_growth_and_structure_of_crystalline_and_amorphous_organic_thin_films_the_case_of_ptylene_and_alpha-NPD). Results and discussion

Measured reflectivities of neutrons and X-ray beams are presented below. The investigated initial structure is $\text{Al}_2\text{O}_3/\text{Nb}(100\text{nm})/\text{Gd}(3\text{nm})/\text{V}(70\text{nm})/\text{Nb}(15\text{nm})$, where Al_2O_3 is a substrate. There is a heterostructure of the S/F/S sandwich, where superconducting materials are niobium and vanadium between which is the ferromagnetic layer of gadolinium with a thickness of 3nm. Due to the mutual impact of superconductivity and ferromagnetism, both superconducting layers (V and Nb) are divided into two sublayers. Because ferromagnetism from the Gd layer affects and changes magnetization profiles in both superconducting layers. Following is a discussion on the influence of different grazing angles of the neutron beam, collinear and non-collinear magnetization, ferromagnetic layer thickness, different ferromagnetic materials, superlattice, and influence of roughness on the neutron and X-ray reflectivity profiles.

1.6.Task 2. Comparing reflectivity at different grazing angles (calculation only neutron reflectivity)

First, we analyze the influence of neutron beam grazing angle on the neutron reflectivity on $\text{Al}_2\text{O}_3/\text{Nb}(100\text{nm})/\text{Gd}(3\text{nm})/\text{V}(70\text{nm})/\text{Nb}(15\text{nm})$ heterostructure. Chosen grazing angles are 3, 6, 9, and 12 mrad, Figure 11.

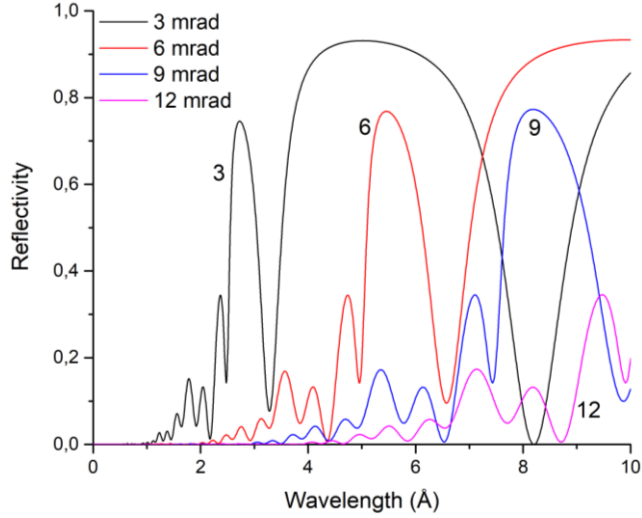


Figure 11. The reflectivity of $\text{Al}_2\text{O}_3/\text{Nb}(100\text{nm})/\text{Gd}(3\text{nm})/\text{V}(70\text{nm})/\text{Nb}(15\text{nm})$ heterostructure for grazing angles of 3, 6, 9, and 12 mrad.

Due to reflection, neutrons change their momentum which depends on the incident angle of the neutron beam, Eq. 1. So with the bigger angles, there is a smaller wavelength of reflected neutrons so the reflectivity spectra are moving to the higher values of the neutron wavelengths as can be seen in Figure 11. We can see that with the increasing of the grazing angle, the intensity of reflectivity decreases, pink line in Figure 11 corresponds to the grazing angle of 12 mrad. The same trend occurs for the transmission spectra, which are given in Figure 12.

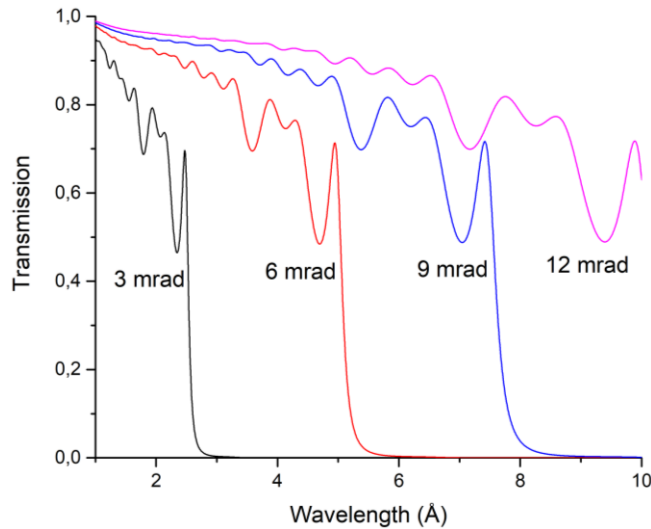


Figure 12. Transmission of $\text{Al}_2\text{O}_3/\text{Nb}(100\text{nm})/\text{Gd}(3\text{nm})/\text{V}(70\text{nm})/\text{Nb}(15\text{nm})$ heterostructure for grazing angles of 3, 6, 9, 12 mrad.

In Figure 11. it can be seen just one reflectivity curve for all samples because R_{++} and R_{--} are almost the same. There is no spin asymmetry because there is no magnetization in the system and so R_{-+} and R_{+-} are equal to zero. The Figure 13. shows spin asymmetry for the case of 6 mrad grazing angle. For all analyzed grazing angles spin asymmetry is of 10-12 orders of magnitudes so it can be concluded that it is negligibly small.

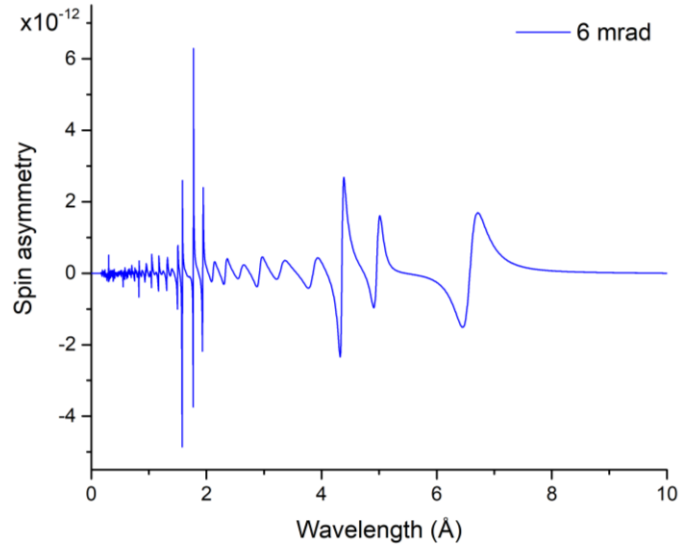


Figure 13. Spin asymmetry for heterostructure, grazing angle of 6 mrad.

1.7.Task 3. Comparing reflectivity at different magnetization (calculation only neutron reflectivity)

Next, we analyzed the dependence on the strength of magnetization and its direction. Reflectivity spectra are shown in Figure 14. Magnetization is just in the z -direction which is colinear magnetization, parallel to the surface of the sample, with values from 100 to 50,000 Oe. For the weakest M_z , a match of R_{++} and R_{--} can be seen, and there is no spin asymmetry, Figure 14. With the increase of the M_z , R_{++} and R_{--} become more and more different in shape and values so spin asymmetry occurs. Higher magnetization has a stronger effect on the neutrons due to the interaction between external magnetization and neutron magnetic moment and thus reflectivity of differently polarized neutrons occurs as evidence of the presence of the magnetic moment.

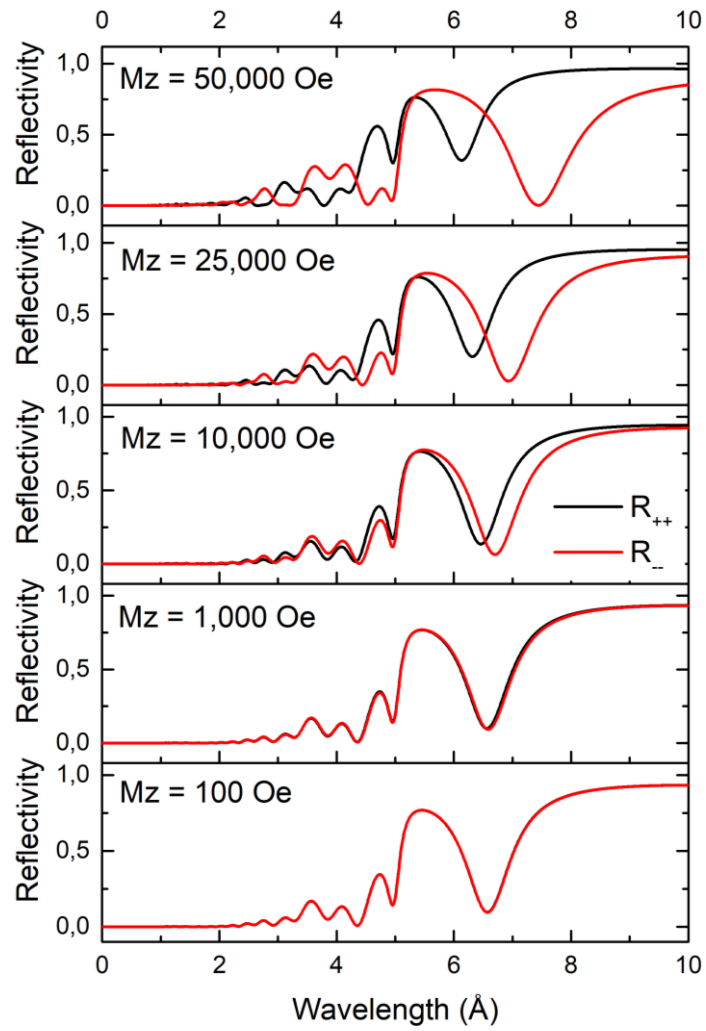


Figure 14. Reflectivities of the same heterostructure in different magnetizations. Magnetizations along x-axis are of 100, 1000, 10,000, 25,000, and 50,000 Oe.

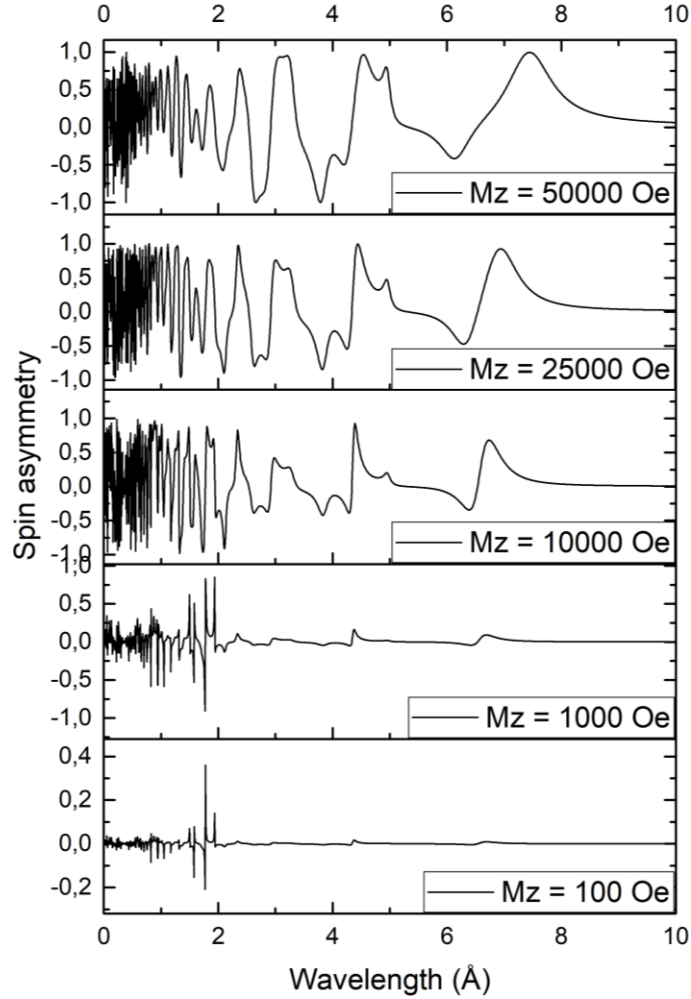


Figure 15. Spin asymmetry for structures in different magnetic fields with M_z of 100, 1,000, 10,000, 25,000, and 50,000 Oe.,

In Figure 16., reflectivities of investigated heterostructure are presented in the colinear magnetization of $M_x = 100, 500,$ and 1000 Oe and $M_z = 1000$ Oe. The spin asymmetry didn't occur. It can be concluded that the z component of magnetization has the main effect on the reflectivity and that the x component doesn't change the neutron reflectivity.

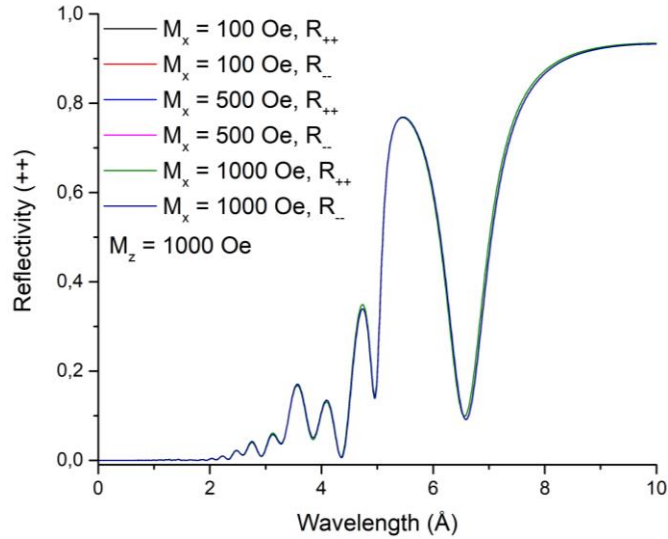


Figure 16. Reflectivity for $M_z = 1000$ Oe, and values M_x of 100, 500, and 1,000 Oe.

1.8. Task 4. Comparing structures with different thicknesses (calculation of neutron and X-ray reflectivity)

The third parameter which we analyze is the thickness of the ferromagnetic layer of gadolinium. The calculation is performed for 3, 6, 9, 12, 15, 20, and 25 nm thick Gd layers. Due to the coherence length of superconductivity, this layer mustn't be too thick. The depth of the penetration of the superconductivity can be a few nanometers in the ferromagnetic layer. Figure 17. Shows reflectivities for the first four thicknesses.

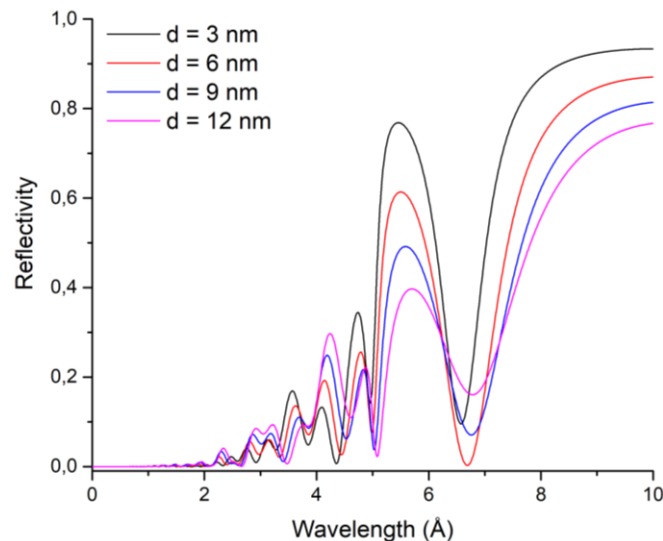


Figure 17. Reflectivity for heterostructure with the Gd layer thicknesses of 3, 6, 9, and 12 nm.

All calculated reflectivities are shown in Figure 18. For the Gd layer thicker than 20 nm there is a change in the shape of reflectivity due to the absorption of neutrons and by analyzing the emitted particles we could get a more detailed spatial magnetic profile of the structure. This is important because the ferromagnet induces magnetic moments in the surrounding superconducting

layers and the profile of the magnetization in them is different close to the interface with the Gd layer.

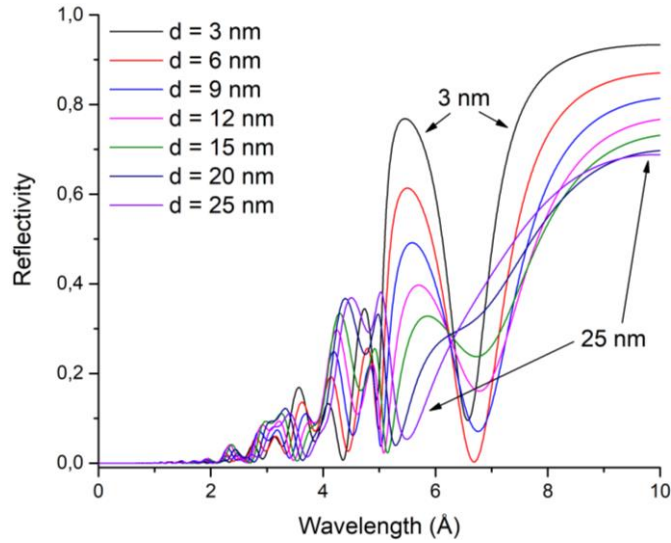
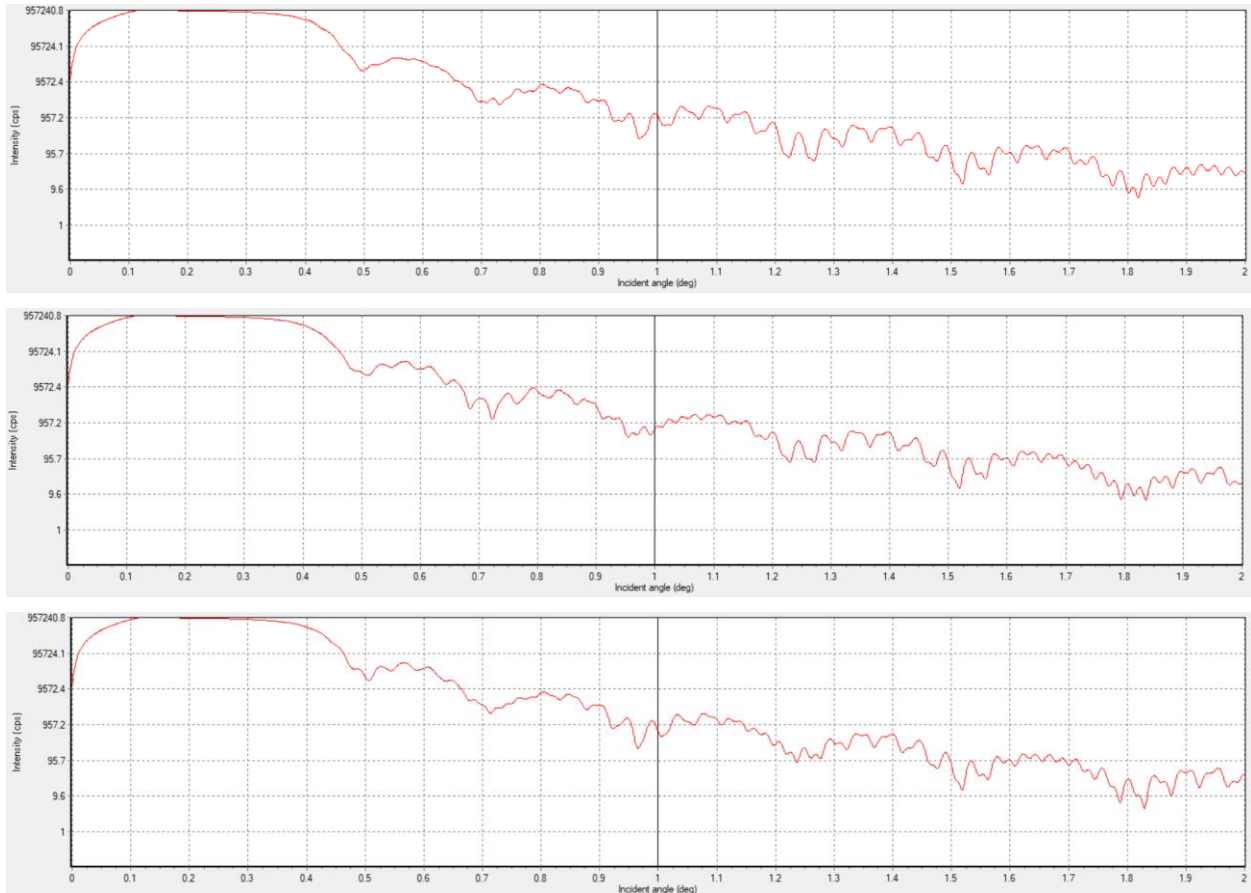


Figure 18. Reflectivity for heterostructure with the Gd layer thicknesses of 3, 6, 9, 12, 15, 20, and 25 nm.

We also calculated X-ray reflectivity which is given in Figure 19. For thicknesses of Gd-layer of 3, 6, 9, and 12 nm. It can be seen that there are no flat surfaces between layers. This is expected due to the small thicknesses of our layers (a few nanometers).



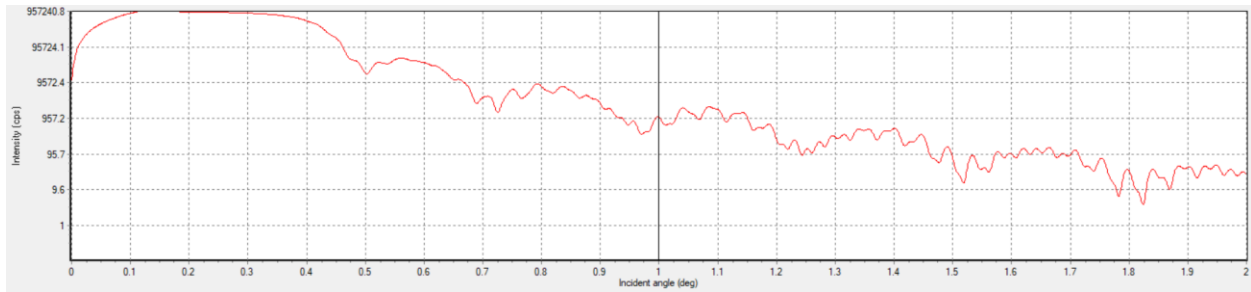


Figure 19. X-ray reflectivities for the heterostructure with the Gd layer thicknesses of 3, 6, 9, and 12 nm.

With the increase of thickness of the Gd layer, there is a change in the "height" of the extremums of the X-ray reflectivity spectra. According to the analysis of their shape and the difference in intensity of these peaks, we can check does Gd layer really has desired roughness and thickness (which is really useful because it is hard to make desired "perfect" nanometer structures).

1.9. Task 5. Comparing structures with different ferromagnets (calculation of neutron and X-ray reflectivity)

There are many different ferromagnet materials so we analyzed both neutron, (Figure 20), and X-ray (Figure 21) reflectivity for the heterostructures with Ni, Fe, Dy, Co, and Gd ferromagnetic layer.

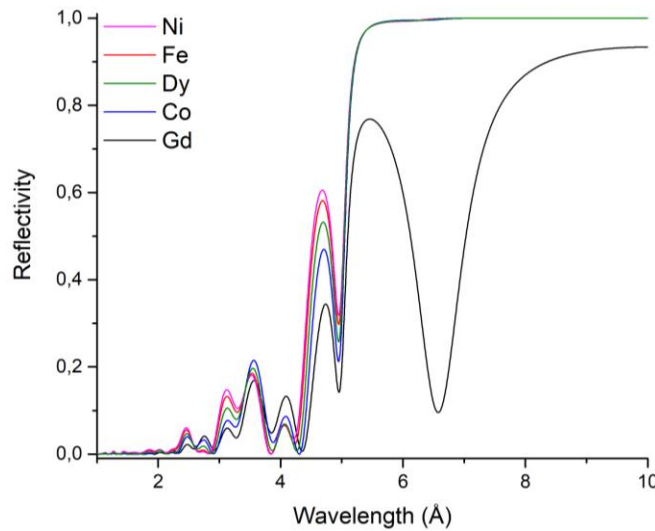
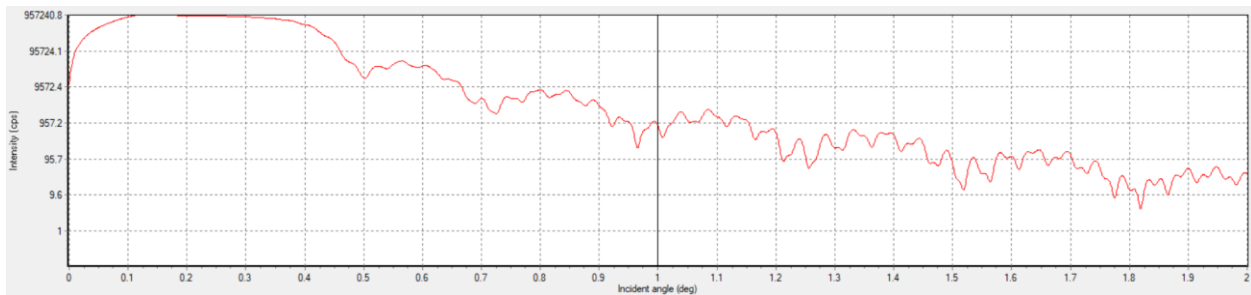


Figure 20. Neutron reflectivity for Co, Gd, Dy, Fe, and Ni.



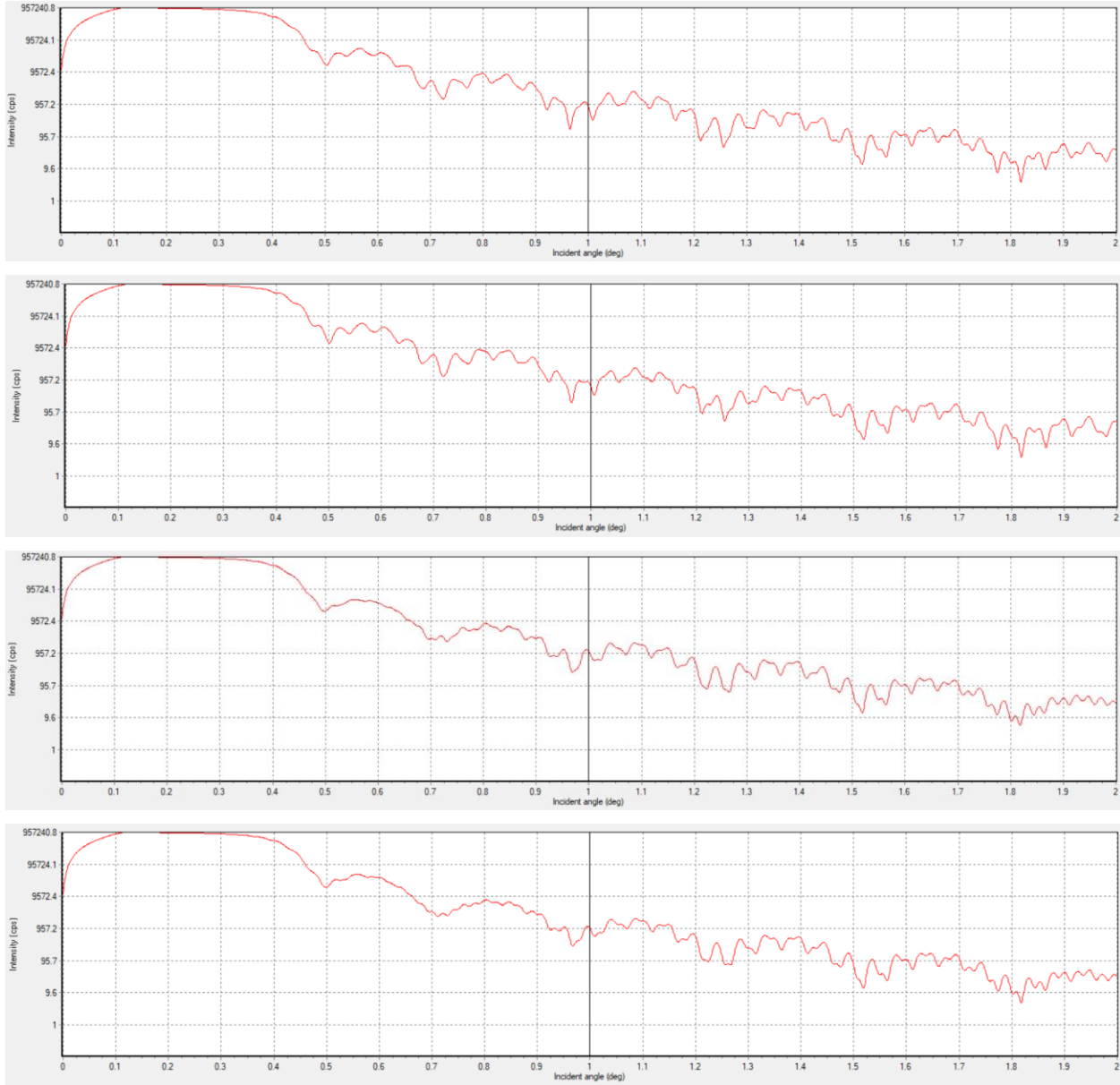


Figure 21. X-ray reflectivities for investigated heterostructures with Fe, Co, Ni, Gd, and Dy ferromagnetic layers, from top to bottom.

When we talk about superconductivity in these metallic layers, we can arrange them in the next array: Co, Gd, Dy, Fe, Ni, from element with lowest to the element with the highest value of coherence length. But when we look at the periodic table of elements, we can arrange them by their mass by following: Fe, Co, Ni, Gd, Dy. In Figure 20, it can be seen that the highest intensity has a reflectivity of the heterostructure with Ni, then Fe, Dy, Co, and on the end Gd. This is not associated nor with their masses (structures and number of neutrons) nor with the coherence length. For neutron reflectivity, there is no any rule for the dependence of the scattering length density of elements on their masses or any other parameter. Different interactions of neutrons with different nuclei (elements) give different angles of the reflection of neutrons. We can just say that neutrons pass by nuclei in the materials with probability which depends on the distance between neutrons and nuclei. Opposite to this, for X-ray reflectivity, there is a law that reflectivity depends directly

on the atomic number of elements, so the reflectivity spectra are correlated with the interaction of X-ray beams and nuclei of elements. In Figure 21. X-ray spectra are arranged like analyzed elements in the period table of elements. It can be seen that with an increase of mass of an element, extremums are more smooth with less small maximums and minimums which are correlated with the roughness of the surface on which reflection takes place.

1.10. Task 6. Superlattice (calculation of neutron and X-ray reflectivity)

In this chapter, we analyze $\text{Al}_2\text{O}_3/[\text{Nb}(25\text{nm})/\text{Gd}(3\text{nm})]_n/\text{Nb}(15\text{nm})$ heterostructures with $n = 10, 20,$ and 30 number of $\text{Nb}(25\text{nm})/\text{Gd}(3\text{nm})$ bilayers. Obtained reflectivities of neutrons and X-ray beams are given in Figures 22, 23, and 24. The neutron reflectivity spectra were given in two ways to make it easier to see the difference between them and to make the results clearer.

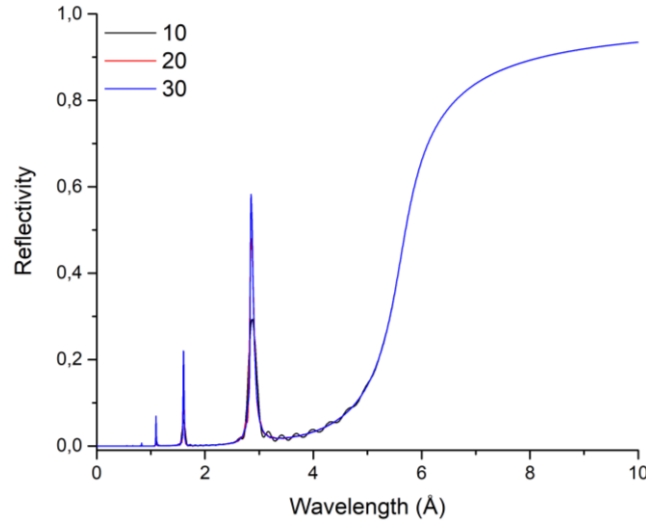


Figure 22. The reflectivity of investigated heterostructure with different superlattices.

Superlattice is made by the different number of bilayers of $\text{Nb}(25\text{nm})/\text{Gd}(3\text{nm})$ layers. The more pairs of these layers exist in the structure, the more intense the reflection maxima due to stronger coupling of ferromagnetism and superconductivity which is happening due to the pairing of electrons from these layers into pairs. One of the electrons is in the F layer and the second one in the S layer but with opposite oriented spin. From Figure 23, it can be seen that for the $n = 30$, the reflectivity curve is smoother.

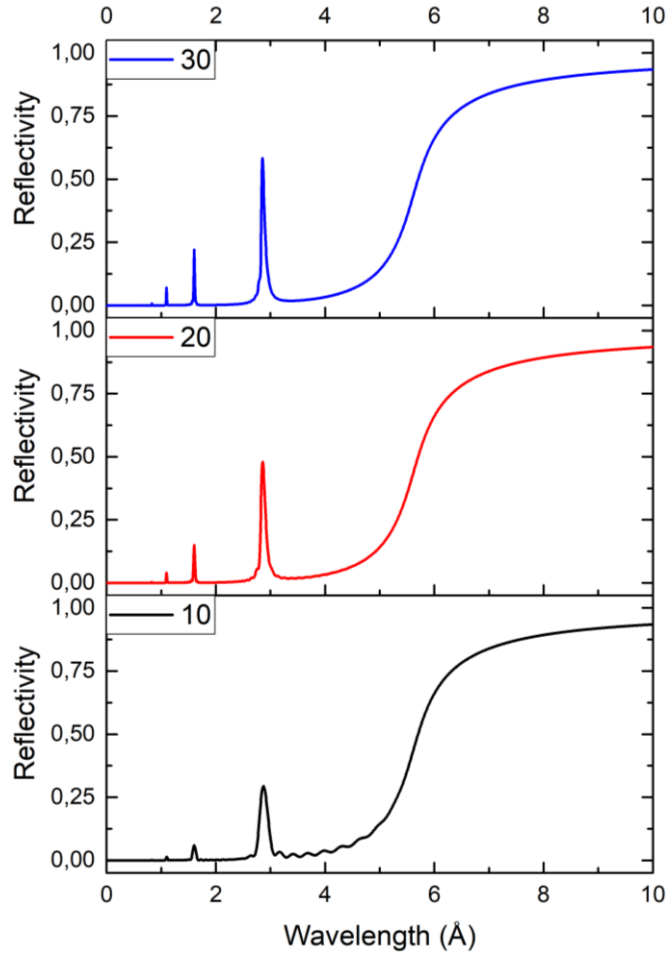
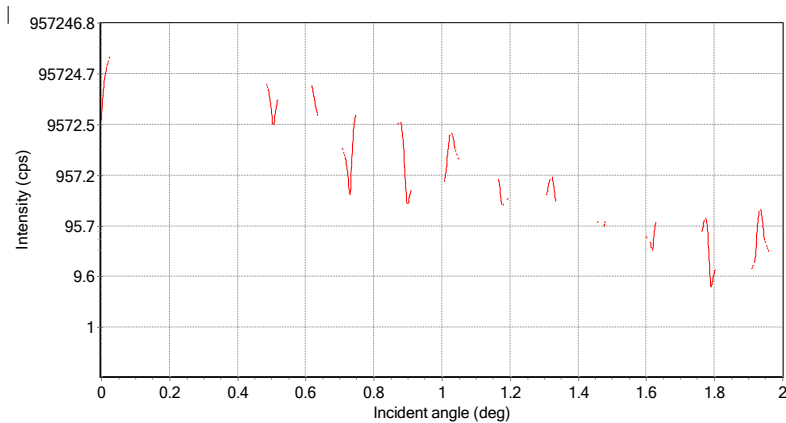


Figure 23. Comparison of the reflectivities of investigated heterostructure with different superlattices.

In Figure 10, it is shown that from the X-ray spectra it is possible to obtain the thickness, density, and roughness of the material. Here we can see small differences in spectra for different numbers of Nb(25nm)/Gd(3nm) bilayers. For $n = 10$, we have at least a smooth reflectivity curve compared to $n = 20$ and 30 . It can also be seen that peaks are of similar intensity for all values of n . So we can conclude that by increasing the number of layers, there are no big differences in X-ray spectra due to small X-ray penetration depth for metallic materials.



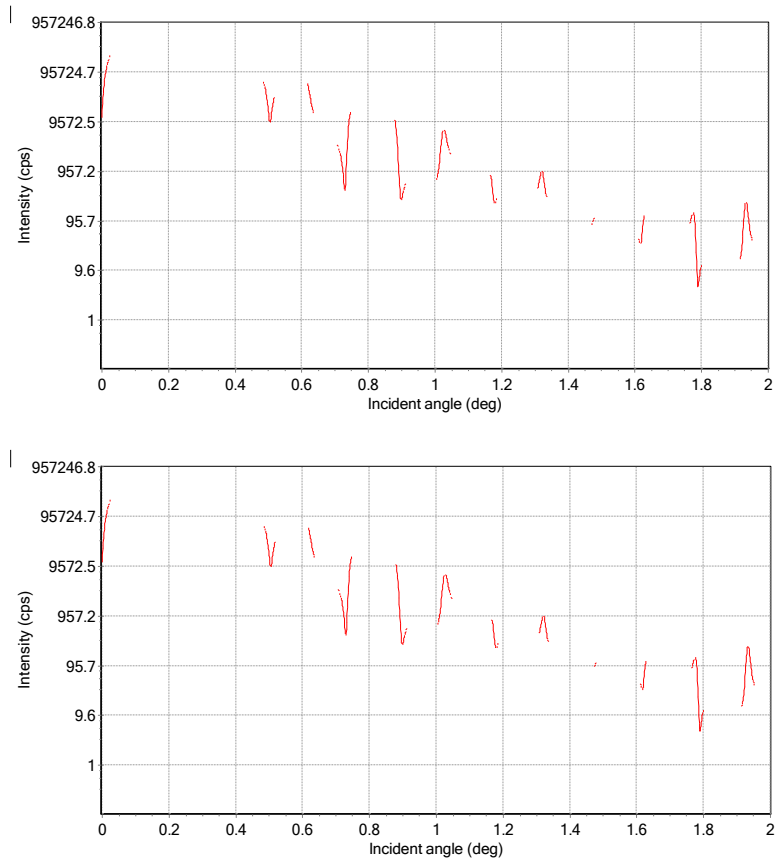


Figure 24. X-ray reflectivities for $Al_2O_3/[Nb(25nm)/Gd(3nm)]_n/Nb(15nm)$ heterostructures with $n = 10, 20,$ and 30 number of $Nb(25nm)/Gd(3nm)$ bilayers, from top to the bottom.

1.11. Task 7. Influence of roughness (calculation only X-ray reflectivity)

Like it is mentioned above, the penetration of X-ray beams in metallic material is small so it interacts on the surface and we can discuss the roughness of the layers. The X-ray spectra for different roughness of 0, 1, 2, and 3 nm for the $Al_2O_3/[Nb(25nm)/Gd(3nm)]_{20}/Nb(15nm)$ heterostructure are shown in Figure 25.

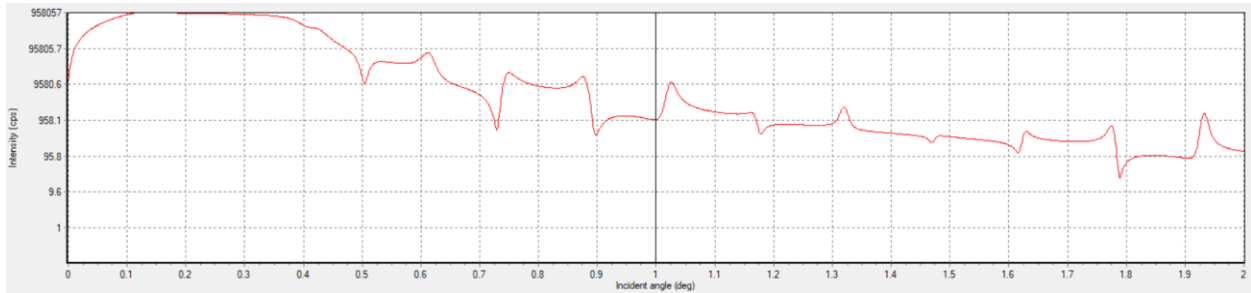




Figure 25. X-ray reflectivities for investigated heterostructures with the roughness of Gd layer of 0, 1, 2, and 3 nm, from top to bottom.

The thickness of the Gd layer is 3 nm and the analyzed roughness is from 0 to 3 nm. We can conclude from this figure and the other before this, that all analyzed structures have layers that are not totally homogenous and there is a mixing of them on the interfaces between neighbor layers. So there can be different degrees of roughness. Figure 25 shows that for a more rough surface, the reflection of X-rays is on different planes in the structure due to the nonhomogenous structure and nonperfect lattice of the metallic layer.

2. Conclusion

In this report, different variations of the parameters and properties of the $\text{Al}_2\text{O}_3/\text{Nb}(100\text{nm})/\text{Gd}(3\text{nm})/\text{V}(70\text{nm})/\text{Nb}(15\text{nm})$ heterostructures are studied from the side of the ferromagnetic/superconducting proximity effect by neutron and X-ray reflectivity. Due to the complexity of the mutual impact of F and S in examined heterostructures, we can conclude that there are present both proximity and inverse proximity effects.

Comparing neutron and X-ray reflectivity spectra, we discussed the influence of the grazing angle of the incident neutron beam, colinear and non-collinear magnetization, thickness of the ferromagnetic layer, different ferromagnetic materials, roughness, and the size of the superlattice on the S/F proximity effect in this structure. There is a big influence on the grazing angle which should be less than 12 mrad. The presence of the magnetization in the system induce spin

asymmetry - the difference between R_{++} and R_{--} reflectivities. Increasing the thickness of the ferromagnetic layer can totally change the shape and intensity of the reflectivity spectra and due to it, there is no significant S/F proximity effect due to short coherence and London penetration lengths. Different ferromagnetic materials give much different reflectivity spectra due to different interactions of elements with neutron and X-ray beams due to different electronic and nuclei structures. The number of the sublayers in the superlattice affects the intensity of peaks in neutron reflectometry but it doesn't give big changes in X-ray reflectivity curves. The roughness of the Gd layer is studied by X-ray reflectometry and it can be obtained from the height of the reflectivity curve peaks.

In the end, it can be concluded that polarized neutron reflectometry is a really powerful technique for analyzing the S/F proximity effects in S/F heterostructures.